

A Study of the Unusual Z Cam Systems IW Andromedae and V513 Cassiopeia*

Paula Szkody^{1,2}, Meagan Albright¹, Albert P. Linnell¹, Mark E. Everett³, Russet McMillan⁴, Gabrelle Saurage⁴, Joseph Huehnerhoff⁴, Steve B. Howell^{5,2}, Mike Simonsen⁶, Nick Hunt-Walker¹

ABSTRACT

The Z Cam stars IW And and V513 Cas are unusual in having outbursts following their standstills in contrast to the usual Z Cam behavior of quiescence following standstills. In order to gain further understanding of these little-studied systems, we obtained spectra correlated with photometry from the AAVSO throughout a 3-4 month interval in 2011. In addition, time-resolved spectra were obtained in 2012 that provided orbital periods of 3.7 hrs for IW And and 5.2 hrs for V513 Cas. The photometry of V513 Cas revealed a regular pattern of standstills and outbursts with little time at quiescence, while IW And underwent many excursions from quiescence to outburst to short standstills. The spectra of IW And are similar to normal dwarf novae, with strong Balmer emission at quiescence and absorption at outburst. In contrast, V513 Cas shows a much flatter/redder spectrum near outburst with strong HeII emission and

*Based on observations obtained with the Apache Point Observatory (APO) 3.5-meter telescope, which is owned and operated by the Astrophysical Research Consortium (ARC).

¹Department of Astronomy, University of Washington, Box 351580, Seattle, WA 98195; szkody@astro.washington.edu

²Visiting Astronomer, Kitt Peak National Observatory, National Optical Astronomy Observatory, which is operated by the Association of Universities for Research in Astronomy (AURA) under cooperative agreement with the National Science Foundation

³National Optical Astronomy Observatories, 950 N. Cherry Ave, Tucson, AZ 85719

⁴Apache Point Observatory, Sunspot NM 88349

⁵NASA Ames Research Center, Moffett Field, CA 94035

⁶49 Bay State Road, Cambridge, MA 02138; mikesimonsen@aavso.org

²Visiting Astronomer, Kitt Peak National Observatory, National Optical Astronomy Observatory, which is operated by the Association of Universities for Research in Astronomy (AURA) under cooperative agreement with the National Science Foundation

prominent emission cores in the Balmer lines. Part of this continuum difference may be due to reddening effects. While our attempts to model the outburst and standstill states of IW And indicate a mass accretion rate near $3 \times 10^{-9} M_{\odot} \text{yr}^{-1}$, we could find no obvious reason why these systems behave differently following standstill compared to normal Z Cam stars.

Subject headings: stars:binaries: close — stars: individual: IW And, V513 Cas
— stars: novae, cataclysmic variables

1. Introduction

Cataclysmic variables (CVs) are close binary systems in which a cool secondary star fills its Roche lobe and transfers mass to a white dwarf primary (Warner 1995). The CVs that undergo outbursts related to their mass transfer rate and subsequent accretion rate onto the white dwarf are termed dwarf novae. The Z Cam systems are a subgroup which generally have relatively long orbital periods (3-5 hrs), relatively high mass transfer and accretion rates and relatively low amplitude (3 mag) outbursts compared to the majority of dwarf novae. The major identifying trait of the Z Cam systems is that they show standstills in their light curves when they remain at about 0.7 magnitude below their outburst brightness for weeks to months. A number of review articles describe a model for dwarf nova outbursts and an explanation for the Z Cam phenomena; e.g. Smak (1984), Cannizzo (1993), Osaki (1996), Lasota (2001), Buat-Ménard et al. (2001a,b).

The basic premise behind standstills is that there is a critical rate of mass accretion that determines outburst behavior. This critical rate is model dependent but depends on the parameters of disk radius, viscosity, orbital period and mass ratio of the system. The systems with rates below the critical value (estimated to be $< 3 \times 10^{-9} M_{\odot} \text{yr}^{-1}$ by Buat-Ménard et al. 2001b for Z Cam) have dwarf nova outbursts while those above the critical rate are novalike systems that remain in a constant high state. The Z Cam systems are thought to be very close to the critical rate. An increase in mass transfer can heat the outer edge of the accretion disk and decrease the critical accretion value so that the disk stays in a stable high state. By taking into account the mass transfer stream-impact on the disk and tidal torques, Buat-Ménard et al. (2001b) were able to reproduce standstills with mass transfer variations of a factor of two for Z Cam. Hartley et al. (2005) compared FUSE observations at quiescence with ORFEUS standstill data on Z Cam itself and showed that the standstill accretion rate of $1 \times 10^{-9} M_{\odot} \text{yr}^{-1}$ was consistent with a lower critical value at standstill than at outburst.

Recently, Simonsen (2011) coordinated an observing campaign (Z CamPaign) that utilized the AAVSO to correctly classify Z Cam systems and monitor their long term light curves. He identified two systems with peculiar behavior following a standstill, IW And and V513 Cas. While the majority of Z Cam systems decline to quiescence after a standstill, these systems usually showed a rise to outburst after standstill. In an attempt to understand this peculiarity and determine the characteristics of these two systems, we obtained spectra at different outburst states throughout a 3-4 month interval in 2011 as well as time-resolved spectra in 2012 to determine the orbital periods of these little-studied systems. We also made an attempt to model the spectra of IW And from quiescence to outburst to find the corresponding accretion rates in comparison to those for Z Cam.

2. Observations

The spectra were obtained at Kitt Peak National Observatory (KPNO) and at the Apache Point Observatory (APO). At KPNO, the RC-Spectrograph was used on the Mayall 4m telescope with the 2048 CCD T2KA and a 1 arcsec slit. Grating KPC-22b in second order enabled a spectrum with good focus from 3800-4900Å with a resolution of 0.7Å pixel⁻¹. Standard stars as well as FeAr lamps were taken for flux and wavelength calibrations. At the 3.5m APO telescope, the Double-Imaging Spectrograph was used in either low (L) or high (H) resolution mode to provide simultaneous blue and red spectral coverage. The low resolution gratings provided useful coverage from 3400-9500Å with a resolution of 1.2Å pixel⁻¹ in the blue and 2.3Å pixel⁻¹ in the red. The high resolution gratings enabled a resolution of 0.6Å pixel⁻¹ over wavelengths of 3900-5000Å in the blue and 6000-7200Å in the red. Flux standards and HeNeAr lamps were used for calibration.

Tables 1 and 2 summarize the observations that were obtained.

For both datasets, IRAF¹ routines were used to accomplish bias and flat field corrections and to transpose the observed data to wavelength and flux. For the high resolution time-resolved spectra obtained during 2012 October, velocity curves were obtained by measuring the emission lines of H α and H β with the centroid *e* routine in *splot* and using an IDL program to find the best fit of the velocities to a sine-curve.

For each observation, the state of the system was obtained from the American Associa-

¹IRAF is distributed by the National Optical Astronomy Observatory, which is operated by the Association of Universities for Research in Astronomy, Inc., under cooperative agreement with the National Science Foundation.

tion of Variable Star Observers² archive and included in Tables 1 and 2. The V magnitudes that are available for each system during 2011 are plotted in Figure 1.

3. Light Curves

The light curves plotted in Figure 1 show the quiescent, outburst and standstill states of each of the two objects. V513 Cas has better coverage and shows four well-defined standstills. In each case, the standstill is followed by a rise to outburst rather than by a decline to quiescence. Unfortunately, the time spent at quiescence is very short and comparison with Table 1 shows that the standstills are well-covered but none of the spectroscopic times coincided with a quiescent state. The time-resolved spectra obtained in 2012 were obtained during the peak of an outburst that followed months at standstill.

IW And (Figure 1) has sparser coverage near the start of the spectroscopic observations. This system has many more excursions to quiescence and Table 2 shows that spectra were obtained at all states. There are two possible standstills, a short one near days 780-790 and a longer one during days 820-840. In each case, the standstill resulted in a rise to outburst. The 2012 October 29 time-resolved spectra were obtained at an interesting time. During the course of the 4.75 hrs of observation, IW And was transitioning to a standstill state following a decline after a brief outburst on October 23 (available AAVSO measurements are V=15.0 on 26 October and V=14.4 on 30 October).

While both objects have roughly 3 mag differences between quiescence and outburst (IW And is 3.4 while V513 Cas is 2.8), and the usual 0.7 mag difference between outburst and standstill, the longer and more frequent standstills apparent in V513 Cas imply its mean mass accretion rate is closer to its critical \dot{M} value.

4. Spectral States

The data acquired in 2011 June over 4-6 consecutive nights (JD2455722-2455727) document the changes that occur from quiescence to outburst in IW And (Figure 2) and through a decline from outburst in V513 Cas (Figure 3). IW And shows the usual spectral changes of dwarf novae from Balmer emission lines at quiescence to deep absorption near outburst as the disk transforms to the hot outburst state. During the rise on June 13, the lag in the rise of the blue light compared to the red is very evident. This lag has been well documented

²<http://www.aavso.org>

from many past studies of dwarf novae, and is evident in both outside-in and inside-out outbursts (Buat-Ménard et al. 2001a). During the last 2 hrs of the 25 spectra obtained on 2012 October 29, the Balmer lines show a rapid transition from emission near quiescence to a standstill configuration with broad absorption flanking strong emission cores (Figure 4). In this rapid rise, the blue continuum flux also seems to lag in the rise.

In contrast to this normal behavior, the spectra of V513 Cas are unusual in the lack of a strong blue continuum near outburst and the weakness of the Balmer emission lines during the decline to quiescence (Figure 3). In addition, the HeII 4686 line is very strongly in emission on the decline from outburst on June 9. As the galactic latitude of V513 Cas is only +3 deg, it is likely that reddening can account for some part of the lack of blue continuum. Since the distance is not known and there is no quiescent spectrum to reveal lines from the secondary star, it is not possible to obtain a value for the reddening. The APO spectra obtained at the peak of outburst on 2012 October 6 (Figure 5) are very similar to the 2011 June 9 spectrum, with the strong HeII line, the emission core in $H\beta$ and a similar rising slope to the red wavelengths. At standstill (Figure 5), the HeII line is still present, although the slope of the continuum flattens out. The standstill spectrum of IW And is also compared to its outburst in Figure 5. Its outburst spectrum is similar but has more blue flux than at standstill.

5. Orbital Period Determination

In order to compare the properties of the two systems in more detail, it was necessary to determine the orbital periods, which relate to the accretion rates and especially the critical rates. Since the 23 time-resolved spectra of V513 Cas were obtained at the peak of outburst and the 25 time-resolved spectra of IW And during a rise to standstill, the blue spectra are difficult to measure due to the broad absorption lines from the accretion disk. However, the red spectra have $H\alpha$ in emission which could be measured and result in the radial velocity curves shown in Figure 6. As many of the IW And blue spectra showed emission lines of $H\beta$ before the standstill state was reached, this line was also measured. The parameters for the least-squares fit of the velocities to a sine-wave are listed in Table 3, where the σ is the standard deviation of the entire fit. For V513 Cas, the 4.3 hrs of spectral coverage was best fit with a period of 312 min (5.2 hrs) while the 4.7 hrs of coverage on IW And yielded a period of 223 min (3.7 hrs). Due to the limited length of the spectral coverage, especially for V513 Cas, these orbital periods should only be used as estimates. However, the values place IW And near the lower limit of Z Cam stars and V513 Cas in the middle (Table 3.2 of Warner 1995). The longer orbital period of V513 Cas implies that its mean

mass transfer/accretion rate and \dot{M}_{crit} are larger than IW And.

6. Modeling IW And

Given the uncertainty in the reddening of V513 Cas and the lower signal-to-noise of its spectra, we chose IW And and the sequence of spectra obtained in 2011 June, as well as the standstill spectra on 29 September, to try to approximate a model for its accretion disk at quiescence, rise, near outburst and standstill. Table 4 contains a list of our adopted system parameters. For consistency with the tables of Knigge (2006) and Knigge et al. (2011), we adopted a white dwarf mass of $0.75M_{\odot}$. With our observed orbital period of 223 min, Figure 16 of Knigge et al. (2011) provides a T_{eff} of 25,000K for the white dwarf. Using this temperature, the radius of a white dwarf with a carbon core and an overlying helium layer is $0.015R_{\odot}$, (Figure 4a of Panei et al. 2000). A secondary mass of $0.27M_{\odot}$ is obtained from Table 3 of Knigge (2006), and results in a mass ratio q of 0.36 for the system. Howell et al. (2001) found that secondary stars with periods longer than 3 hrs have bloated secondaries, which would increase the secondary radius and q values slightly, but the secondary has little effect on the outburst and standstill spectra. The observed radial velocity amplitude constrains the orbital inclination to about 30 degrees. The M_V - P_{orb} relations from Harrison et al. (2004) and Patterson (2011) provide a distance of about 700 pc that is used as a scaling factor between the models and the observed spectra.

Figure 7 presents a projection of the system on the plane of the sky while Figure 8 shows the model radial velocity curves of the two stellar components (the observed velocities shown in Figure 6 are from the emission lines originating in the accretion disk).

We do not have a time-dependent outburst model available to calculate theoretical synthetic spectra as a function of time during an outburst cycle; consequently, we model conditions at outburst and standstill with hot stable disks, with mass accretion rate equal to the mass transfer rate. We therefore used BINSYN (Linnell et al. 2012), which calculates models of stable cataclysmic variables in the hot state, with input annuli calculated with TLUSTY (Hubeny 1988), and SYNSPEC (Hubeny et al. 1994) to model the observed outburst spectrum of 2011 June 14. Under normal operation, BINSYN is supplied with a set of annulus synthetic spectra for a specified mass transfer rate and white dwarf mass. BINSYN then uses the specified mass transfer rate and range of radii in the accretion disk to calculate theoretical T_{eff} values as a function of annulus radius. If there are many more narrow width annuli specified than available synthetic spectra, BINSYN interpolates to the specified annuli T_{eff} values. In addition to calculating a synthetic spectrum for the accretion disk face, BINSYN also calculates a synthetic spectrum for the accretion disk rim and for

the white dwarf and the secondary star (see Linnell & Hubeny 1996, for details).

We used TLUSTY and SYNSPEC to calculate complete steady state accretion discs for mass transfer/accretion rates of 1.0, 2.0, and $3.0 \times 10^{-9} M_{\odot}\text{yr}^{-1}$ with a viscosity parameter $\alpha = 0.10$. In each case we represented the accretion disk with 40 annuli in two groups of equal width annuli. The first group of 10 annuli extended from the white dwarf equator to the radius of maximum T_{eff} at $1.36 R_{wd}$. The second group extended from the first group boundary to the cutoff radius specified by BINSYN. The synthetic spectrum fits to the observational data at outburst are sensitive to the mass transfer rate. Both the rates of 1.0 and 2.0×10^{-9} had too little flux in the 3800-4000Å region while the value of 3×10^{-9} provided the best fit. With the distance specified, the outer radius of the accretion disk was modified by trial and error until the system output synthetic spectrum from BINSYN fitted the outburst spectrum as closely as possible. The outer radius of the standard model accretion disk thus determined was $0.14R_{\odot}$ (1.0×10^{10} cm for the outburst model). The fit to the outburst spectrum is shown in Figure 9 and this disk size is shown in Figure 7.

If we assume the same steady mass transfer/accretion rate exists at all states, the flatter slopes of the rising to outburst and quiescent observed spectra (data from 2011 June 13 and 11 respectively) point to a lower excitation accretion disk. To fit both the continuum and the depths of the Balmer lines in the rising spectrum, a source with T_{eff} of $\sim 13,000\text{K}$ is needed. Consequently, we successively removed the inner highest temperature annuli input to BINSYN until a fit was achieved. This led to the fit shown in Figure 10, with the highest T_{eff} annulus at 12,479K at a distance of $8R_{wd}$ and an outer disk radius of $0.27R_{\odot}$ (1.88×10^{10} cm). While this fit looks quite good, the nature of the disk during the rise to outburst is likely not in a steady state. However, the temperature fits give some measure of the conditions of the disk material during that time.

For the quiescent spectrum, we note the presence of Balmer emission lines suggesting the possibility of an optically thin region of the accretion disk (see the comments by Patterson 2011). On the other hand, Idan et al. (2010) find that quiescent accretion disks are optically thick with a $T_{eff} \sim 5000\text{K}$. We supplied BINSYN with solar composition stellar synthetic spectra for T_{eff} values of 3500K and 7000K for interpolation, and used the BINSYN option to specify explicit T_{eff} values for accretion disk annuli; we specified 5000K for the outermost 32 annuli and 6000K for the innermost 8 annuli. The reason for the slight temperature gradient was to produce a slightly flatter continuum for comparison with the observed spectrum. Since the annulus T_{eff} values are specified, our result does not depend on a particular viscosity parameter value. The quiescent continuum source cannot have a T_{eff} much above 5000K without producing a discrepancy with the observed continuum slope. The empirical procedure of adjusting the outer radius of the accretion disk to produce a fit to the observed

quiescent spectrum, using the distance scaling factor, led to an outer radius of the accretion disk of $0.08R_{\odot}$. Figure 11 shows this fit along with the contributions of the white dwarf and the secondary star to the quiescent spectrum. The dominance of the accretion disk over that of the underlying stars is confirmed by the lack of any TiO bands or rise in flux evident in the red spectrum obtained at quiescence on 2011 July 5.

Applying a similar method to the standstill spectra from 2011 September 29, using the same set of annuli as the rising to outburst model results in a radius of the disk of $0.33R_{\odot}$. This fit is shown in Figure 12. The model Balmer lines are deeper than observed but the observed lines are filled in by emission cores.

We can compare our values to the best studied system, Z Cam. Hartley et al. (2005) used ultraviolet data from FUSE and ORFEUS to obtain model parameters for the system at quiescence and standstill. They found a white dwarf temperature near 57,000K and a disk at standstill accreting at about $1 \times 10^{-9} M_{\odot} \text{ yr}^{-1}$, which is about a factor of 4 below the accretion rate at outburst (Knigge et al. 1997). The orbital period of Z Cam (7 hrs) is about twice that of IW And so the expectation of a hotter white dwarf and a higher mass accretion rate compared to IW And is reasonable. Since the standstill disk accretion rate was shown to be less than outburst, we attempted to also fit IW And with a reduced rate. Using a mass accretion rate of $1.0 \times 10^{-9} M_{\odot} \text{ yr}^{-1}$ and the hot radii extending to the white dwarf equator results in an outer radius of the accretion disk of $0.16R_{\odot}$. This model fit is shown in Figure 13. The high order Balmer absorption lines are fit better with this lower accretion rate, but the continuum falls off too steeply to provide a good fit at longer wavelengths. Thus, neither of our two models represent the standstill situation well. Given the short wavelength range of our optical data, and the lack of ultraviolet spectra to determine the actual white dwarf T_{eff} , further refinements must await more extensive coverage.

7. Conclusions

Our photometric and spectroscopic monitoring program over 3-4 months has revealed some new information on the little-studied systems of IW And and V513 Cas. IW And is a very variable system, showing constant excursions from quiescence to outburst, with infrequent standstills. In contrast, V513 Cas spends about half its time in a standstill or outburst state, with only brief returns to quiescence about once per month. The spectra of IW And at different states are very typical of dwarf novae, with strong Balmer emission at quiescence and deep Balmer absorption at outburst. While the quiescent state of V513 Cas was not captured, the outburst and standstill states are flat or decreasing to the blue, while the high excitation line of HeII is strongly in emission. Our time-resolved spectra provide

orbital periods near 3.7 hrs for IW And and 5.2 hrs for V513 Cas.

Our modeling efforts on the outburst of IW And indicate a mass accretion rate of $3 \times 10^{-9} M_{\odot} \text{ yr}^{-1}$ for a white dwarf mass of $0.75 M_{\odot}$ and corresponding parameters from relations in the literature for the secondary ($0.27 M_{\odot}$) and a distance of 700 pc. This same rate of mass accretion can fit the rise to outburst and the quiescent spectra if the radius of the disk is altered. The fit to the standstill spectra are not as satisfactory, producing deeper absorption lines than observed. If the accretion rate is lowered by a factor of 3, the continuum is too steep as compared to the observations. Further wider wavelength coverage, especially in the ultraviolet is needed to formulate a better model for the disk. With the data in hand, we could find no obvious reason why the emergence from standstill to an outburst rather than to quiescence occurs in these two systems contrary to the normal Z Cam system. Characterising the basic parameters is just a first step toward a solution to that dilemma.

We acknowledge with thanks the variable star observations from the AAVSO International Database contributed by observers worldwide and used in this research. We are also grateful to Thomas Harrison for obtaining a spectrum as part of this program. This work was partially supported by NSF grant AST-1008734.

Facility: AAVSO, Mayall(RC-Spec), APO(DIS)

REFERENCES

- Buat-Ménard, V., Hameury, J.-M., & Lasota, J.-P., 2001a, A&A, 366, 612
- Buat-Ménard, V., Hameury, J.-M., & Lasota, J.-P., 2001b, A&A, 369, 925
- Cannizzo, J. K., 1993, ApJ, 419, 318
- Hartley, L. E., Long, K. S., Froning, C. S. & Drew, J. E. 2005, ApJ, 623, 425
- Harrison, T. E. et al. 2004, AJ, 127, 460
- Howell, S. B., Nelson, L. A. & Rappaport, S. 2001, ApJ, 550, 897
- Hubeny, I. 1988, Comput. Phys. Comm., 52, 103
- Hubeny, I., Lanz, T., & Jeffery, C. S. 1994, in Newsletter on Analysis of Astronomical Spectra No. 20, ed. C.S. Jeffery (St. Andrews Univ.),30
- Idan, I., Lasota, J.-P., Hameury, J.-M., & Shaviv, G., 2010, A&A, 519, A117

- Knigge, C., 2006, MNRAS, 373, 484
- Knigge, C., Baraffe, I. & Patterson, J. 2011, ApJS, 184, 28
- Knigge, C., Long, K. S., Blair, W. P. & Wade, R. A. 1997, ApJ, 476, 291
- Lasota, J.-P., 2001, NAR, 45, 449
- Linnell, A. P. & Hubeny, I., 1996, ApJ, 471, 958
- Linnell, A. P., DeStefano, P., & Hubeny, I., 2012, PASP, 124, 885
- Osaki, Y., 1996, PASP, 108, 39
- Panei, J. A., Althaus, L. G., & Benvenuto, O. G., 2000, A&A, 353, 970
- Patterson, J. 2011, MNRAS, 411, 2695
- Simonsen, M. 2011, JAAVSO, 39, 66
- Smak, J., 1984, ActaAstr, 34, 161
- Warner, B., 1995, Cataclysmic Variable Stars [Cambridge: University Press]

Table 1. V513 Cas Spectroscopic Observations

UT Date	JD	Obs	Exp(min)	UT Start	V	State
05/14/2011	2455695.5	KPNO	10.4	11:19:09	15.8	standstill
05/15/2011	2455696.5	KPNO	15x2	10:55:30	15.8	standstill
05/16/2011	2455697.5	KPNO	10	11:12:42	15.8	standstill
06/09/2011	2455721.5	KPNO	15	11:01:55	15.4	decline
06/10/2011	2455722.5	KPNO	13.3	11:04:41	-	decline
06/11/2011	2455723.5	KPNO	20	10:31:45	-	decline
06/12/2011	2455724.5	KPNO	15	10:41:09	-	decline
06/13/2011	2455725.5	KPNO	15	10:51:59	16.4	decline
06/14/2011	2455726.5	KPNO	20	10:41:23	16.7	decline
07/05/2011	2455747.5	APO,H	15	09:36:33	15.7	standstill
08/14/2011	2455787.5	APO,L	15	05:38:24	15.8	standstill
08/20/2011	2455793.5	APO,L	6.7x3	07:18:32	15.8	standstill
08/26/2011	2455799.5	KPNO	20	10:43:24	15.8	standstill
08/27/2011	2455800.5	APO,L	6.7x2	07:22:23	15.8	standstill
09/04/2011	2455808.5	KPNO	16.7	10:57:300	15.6	rise
09/16/2011	2455820.5	APO,L	10	06:58:29	15.8	decline
09/29/2011	2455833.5	APO,H	15x2	07:35:38	15.5	decline
10/06/2012	2456206.5	APO,H	10x23	02:37:32	15.2	outburst

Table 2. IW And Spectroscopic Observations

UT Date	JD	Obs	Exp(min)	UT Start	V	State
06/11/2011	2455723.5	KPNO	20	10:55:37	-	quiescence
06/12/2011	2455724.5	KPNO	15	11:00:01	-	quiescence
06/13/2011	2455724.5	KPNO	15	11:10:50	-	rise
06/14/2011	2455726.5	KPNO	15	11:05:31	-	outburst
07/05/2011	2455747.5	APO,H	10	09:54:38	17.2	quiescence
08/14/2011	2455787.5	APO,L	15	06:27:25	15.0	standstill
08/20/2011	2455793.5	APO,L	5x3	07:45:26	15.0	standstill
08/26/2011	2455799.5	KPNO	20	10:19:08	14.0	outburst
08/27/2011	2455800.5	APO,L	5x2	07:45:45	14.0	outburst
09/04/2011	2455808.5	KPNO	20	10:01:18	17.0	quiescence
09/16/2011	2455820.5	APO,L	5	06:48:43	14.7	standstill
09/29/2011	2455833.5	APO,H	10x2	07:13:11	14.5	standstill
10/29/2012	2456229.5	APO,H	10x25	02:03:38	14.4	standstill

Table 3. Radial Velocity Solutions

Object	Line	$\gamma(\text{km s}^{-1})$	$K (\text{km s}^{-1})$	P (min)	$\sigma(\text{km s}^{-1})$
IW And	H α	-13.8 \pm 0.6	46.2 \pm 3.5	223	11
IW And	H β	-61.9 \pm 1.1	57.5 \pm 6.5	221	21
V513 Cas	H α	-35.9 \pm 0.4	42.4 \pm 1.9	312	7

Table 4. IW And System Parameters

Parameter	Value
Period	223 min
WD T_{eff}	25,000K
M_{wd}	$0.75M_{\odot}$
R_{wd}	$0.015R_{\odot}$
M_{sec}	$0.27M_{\odot}$
q	0.36
d	700 pc
i	30°

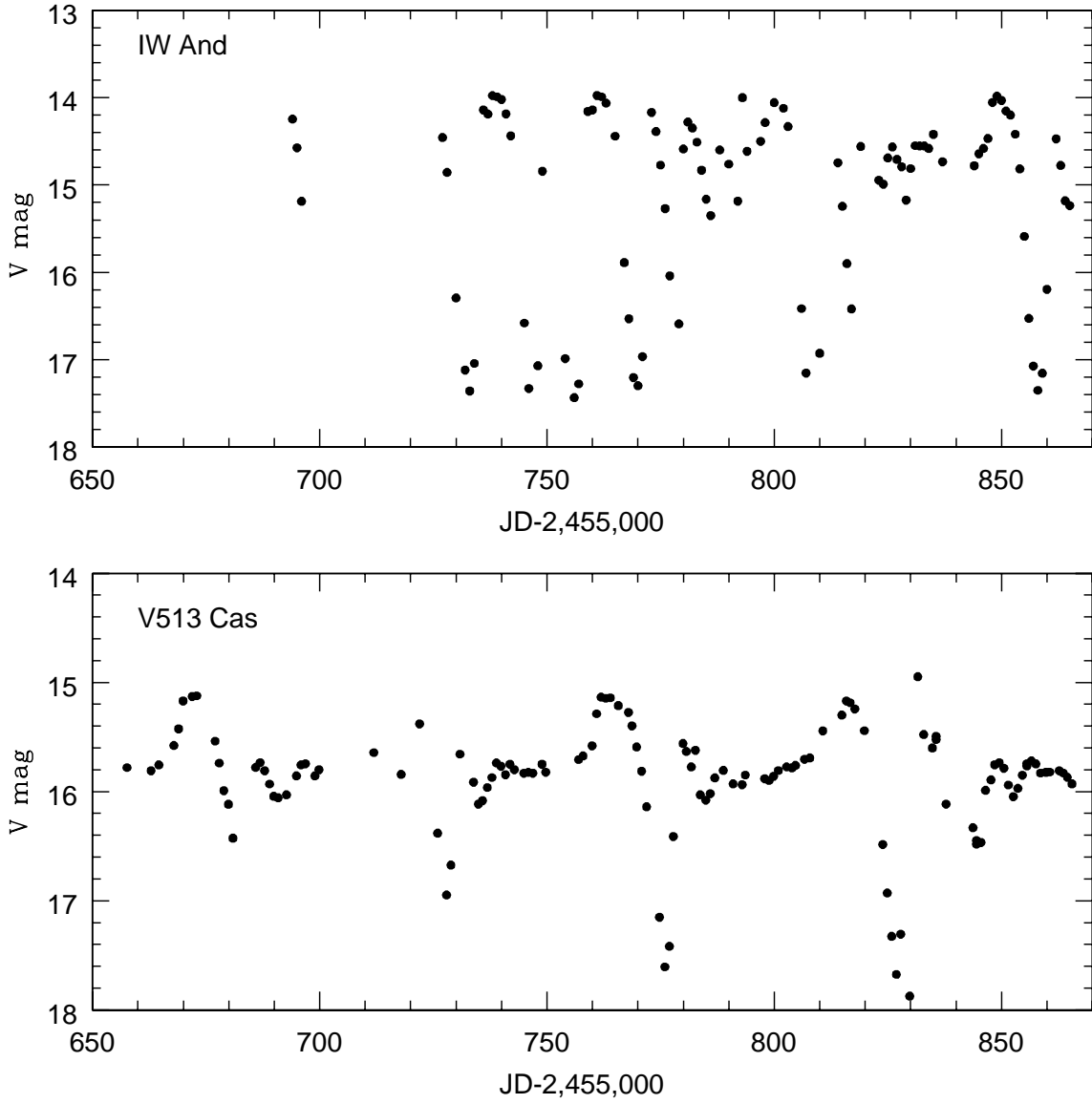


Fig. 1.— AAVSO data during the timespan of our 2011 spectroscopic coverage.

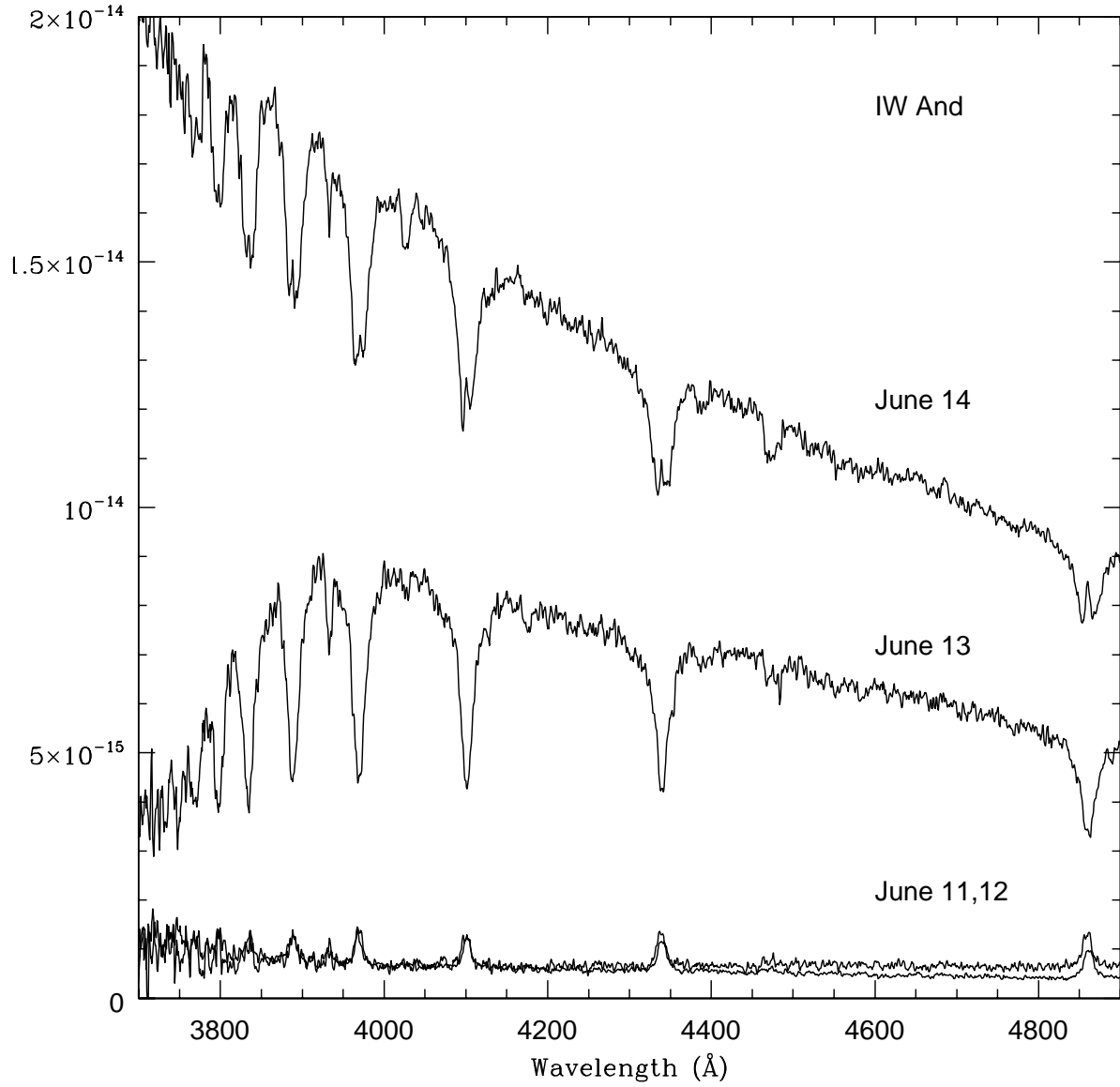


Fig. 2.— KPNO sequence of spectra showing the change in spectra over 3 days when IW And went from quiescence to outburst.

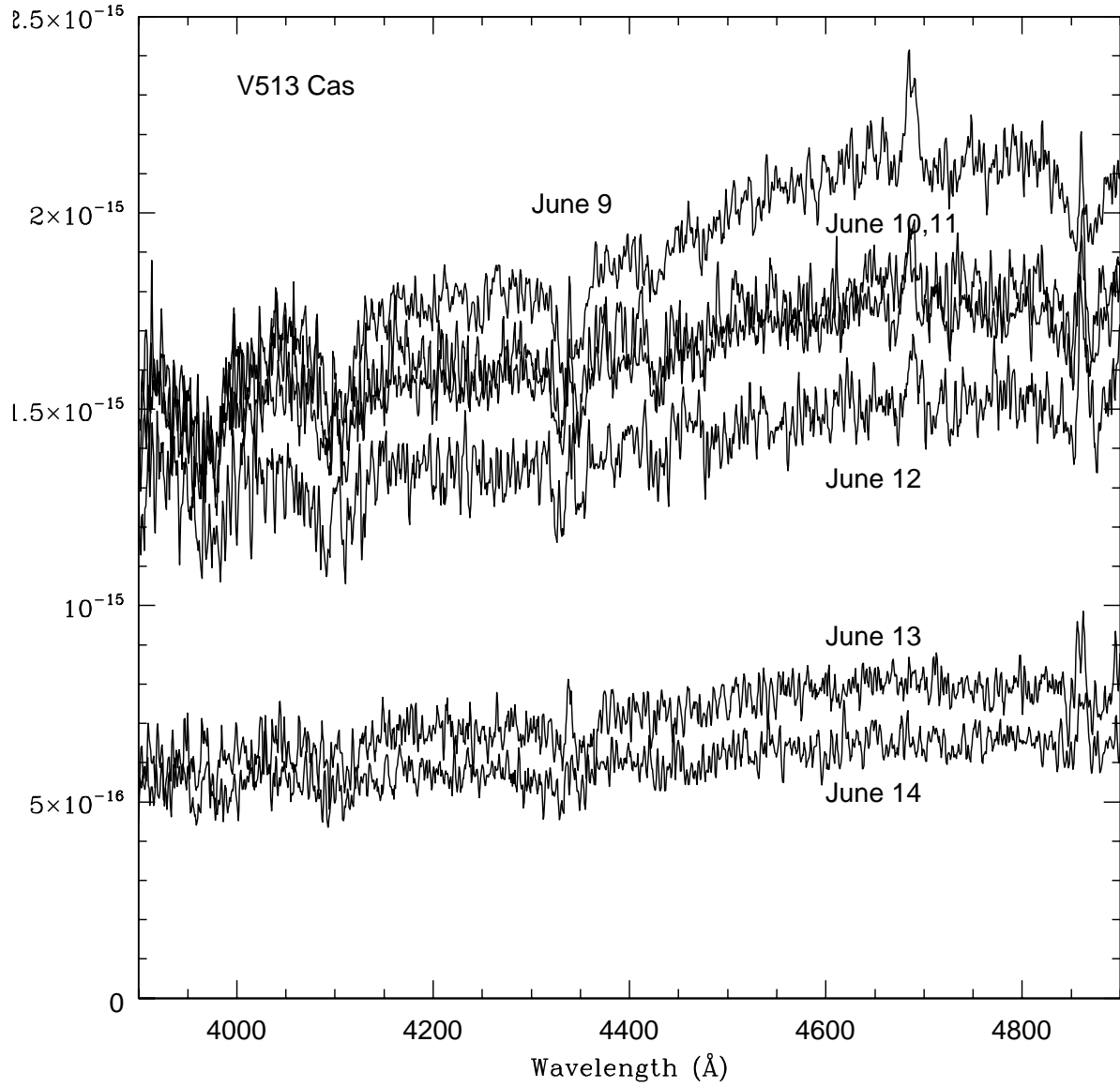


Fig. 3.— KPNO sequence of spectra showing the change in spectra over 5 days as V513 Cas declined from outburst to midway to quiescence.

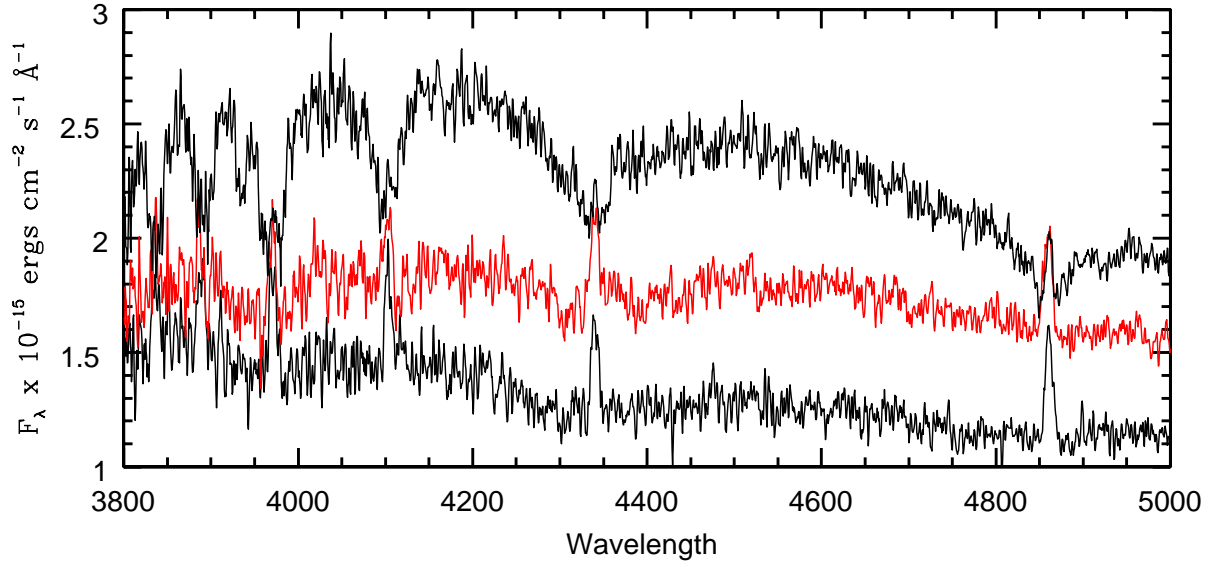


Fig. 4.— APO sequence of spectra showing the change in spectra over the last 2 hrs of 2012 October 29 as IW And changed from declining from an outburst (bottom) to a standstill state (top).

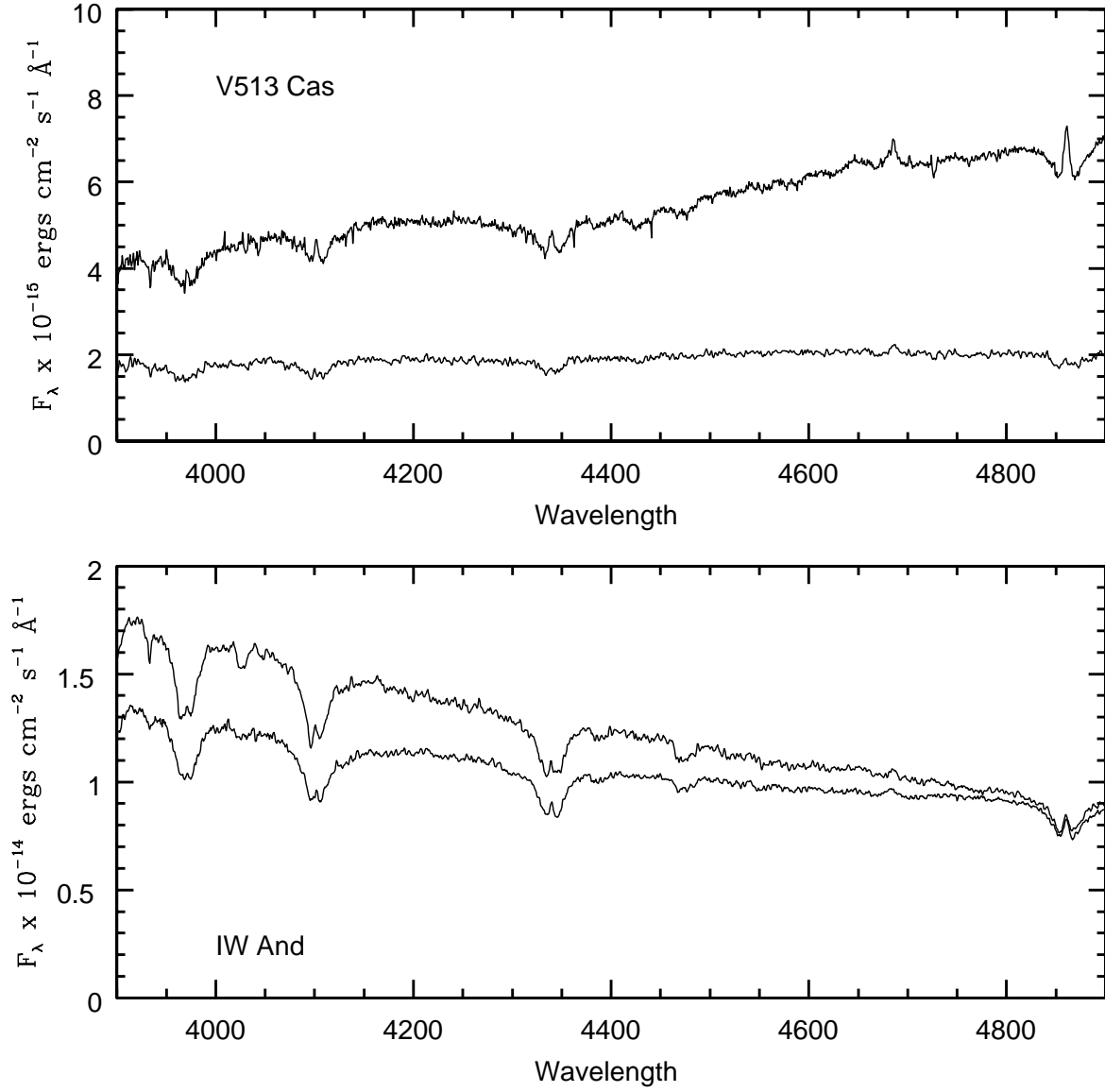


Fig. 5.— Comparison of spectra at outburst and standstill for V513 Cas (2011 May 15 and 2012 October 6) and IW And (2011 June 14 and September 29).

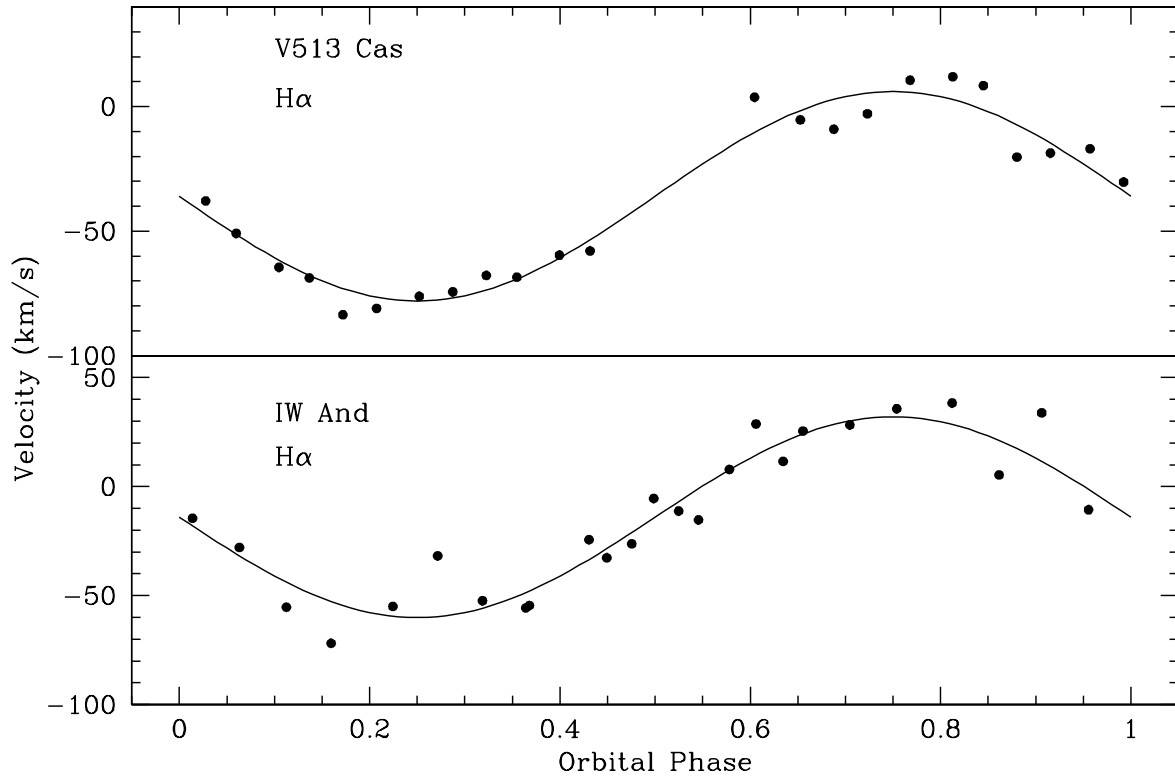


Fig. 6.— H α velocities and best-fit sine-curve solution using the values given in Table 3.

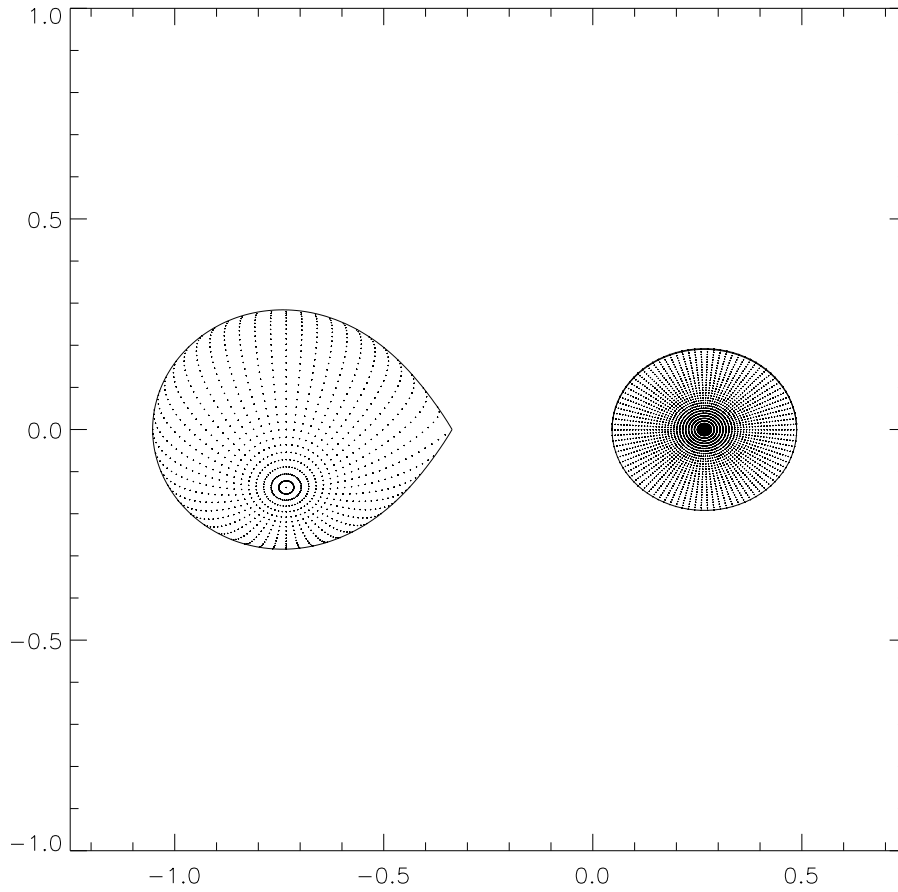


Fig. 7.— View of IW And system model projected on the plane of the sky. The orbital inclination is 30° .

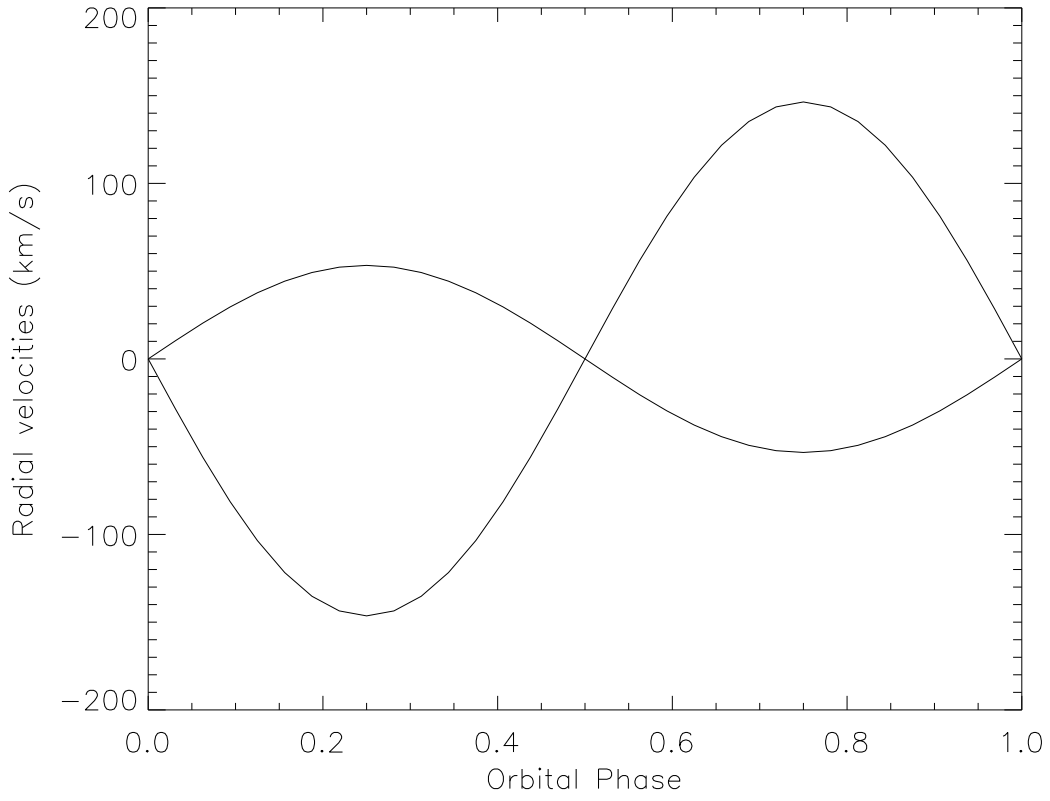


Fig. 8.— Theoretical radial velocity curves of adopted model stellar system components.

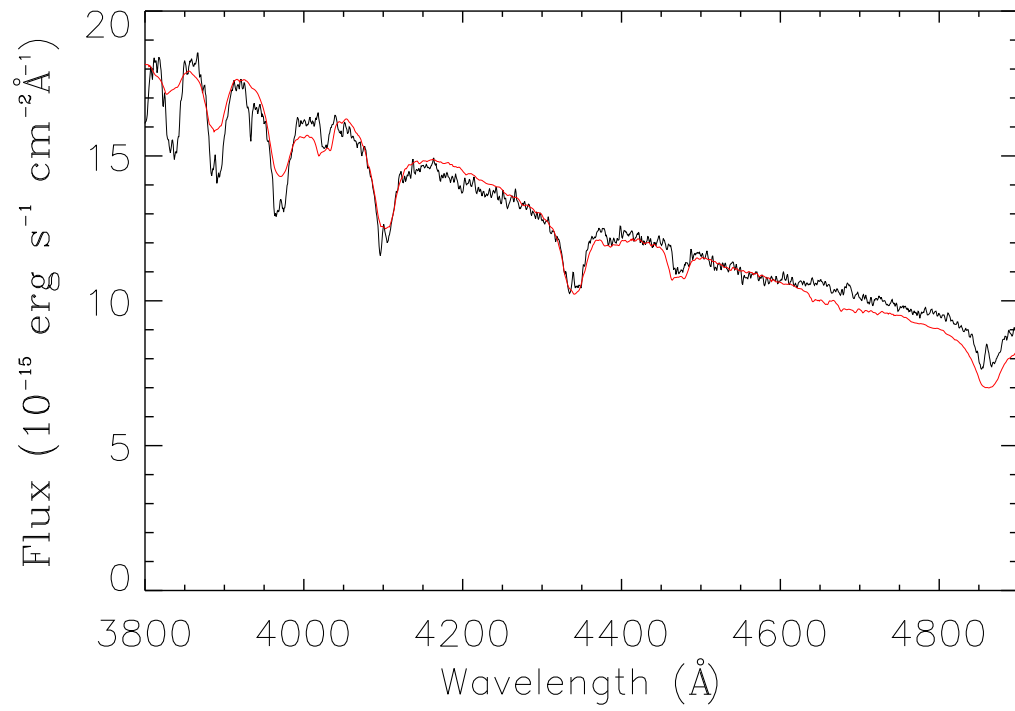


Fig. 9.— Comparison of IW And outburst model (red curve) for mass accretion rate of $3 \times 10^{-9} M_{\odot} \text{ yr}^{-1}$ with observed spectrum (black curve) from 2011 June 14.

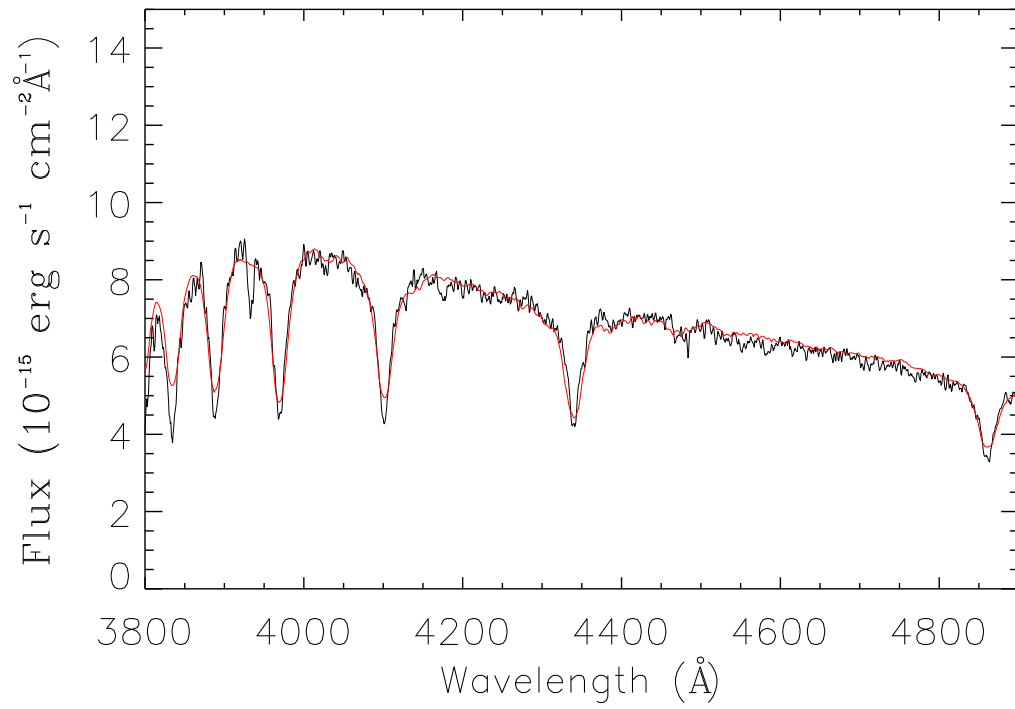


Fig. 10.— Comparison of IW And rising to outburst model for mass accretion rate of $3 \times 10^{-9} M_{\odot} \text{ yr}^{-1}$ with observed spectrum from 2011 June 13.

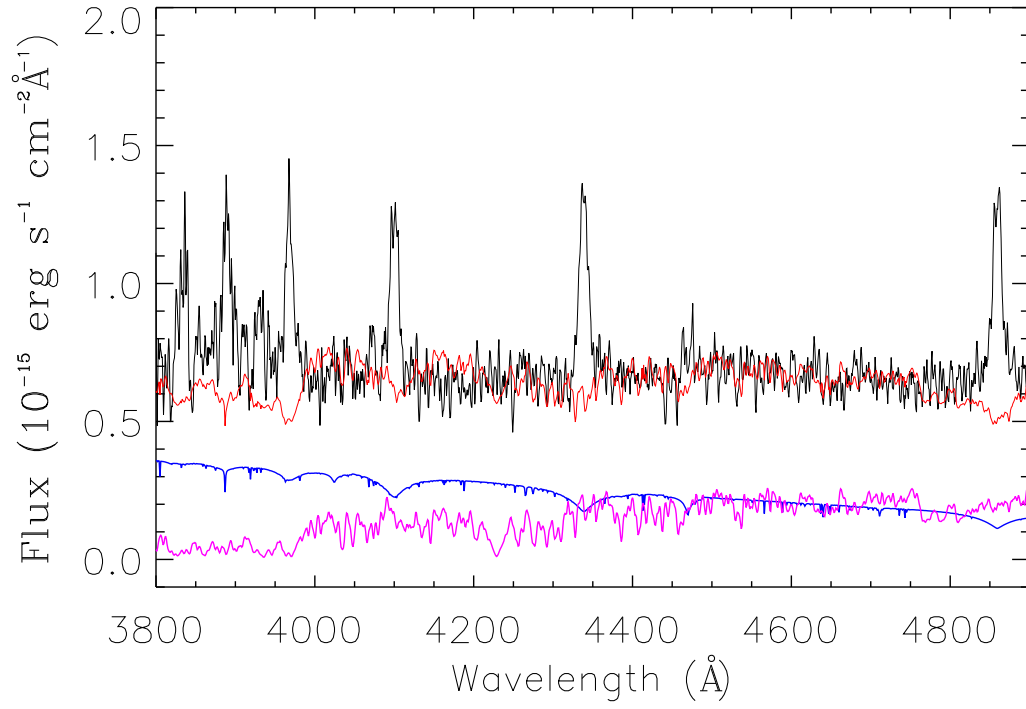


Fig. 11.— Comparison of IW And quiescent model (red) for specified T_{eff} values with observed spectra on 2011 June 11 (black). White dwarf component is shown with blue line and secondary star with magenta line.

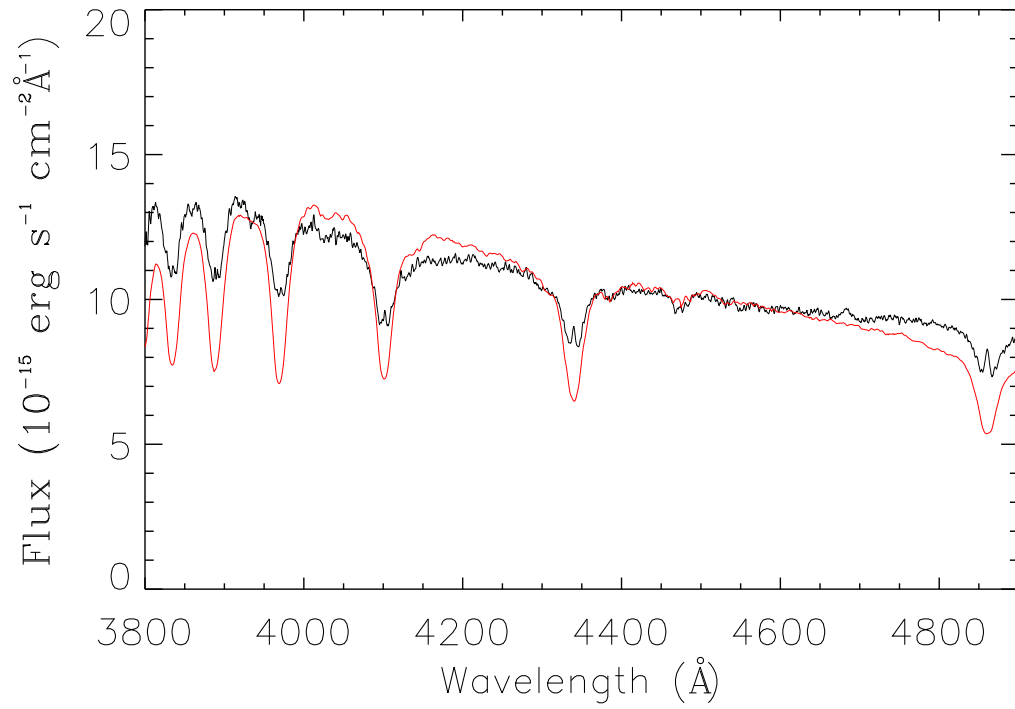


Fig. 12.— Comparison of IW And standstill model for mass accretion rate of $3 \times 10^{-9} M_{\odot} \text{ yr}^{-1}$ with observed spectrum from 2011 September 29.

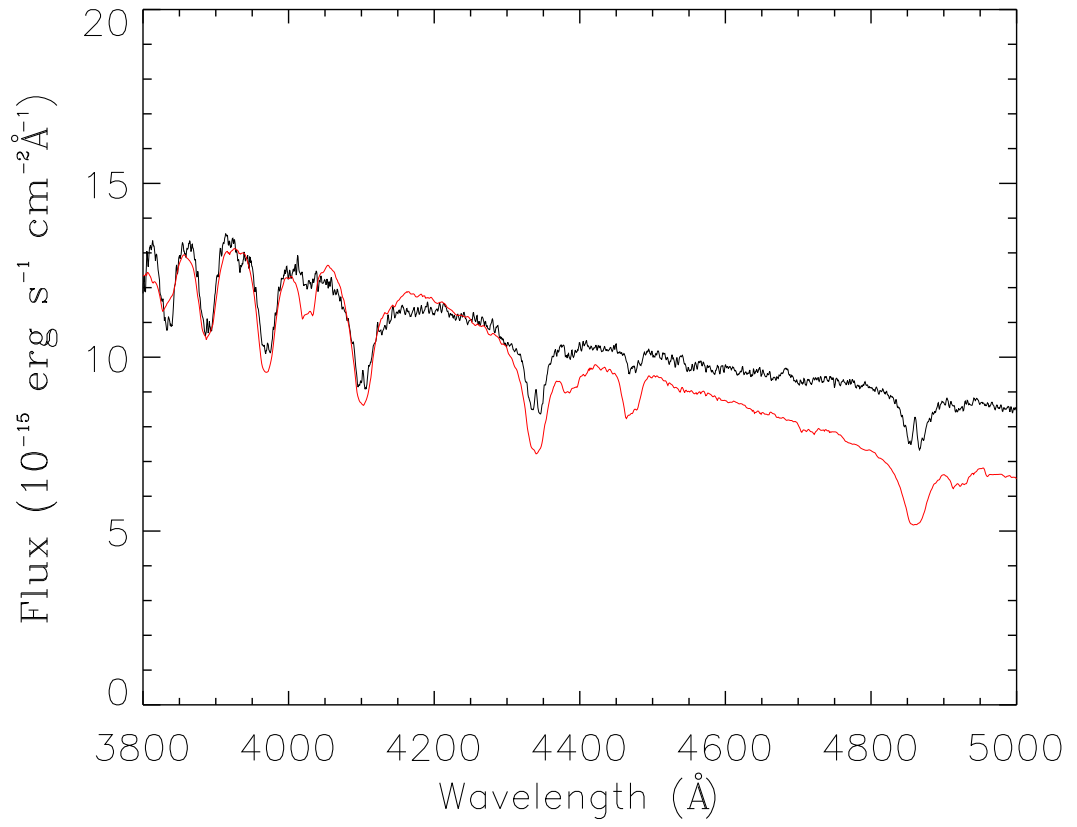


Fig. 13.— Comparison of IW And standstill model for mass accretion rate of $1 \times 10^{-9} M_{\odot} \text{ yr}^{-1}$ with observed spectrum from 2011 September 29.